

Skyrmion-electron bound states in a Néel antiferromagnet

N. Davier^{1,*} and R. Ramazashvili^{1,†}

¹*Laboratoire de Physique Théorique, Université de Toulouse, CNRS, UPS, France*

(Dated: August 9, 2022)

We show that, in a Néel antiferromagnet with a particular location of electron band extrema, a Skyrmion and an electron form bound states with energy of the order of the gap Δ in the electron spectrum. The bound states turn the Skyrmion into a charged particle, that can be manipulated by electric field.

Introduction — Topological textures such as domain walls, vortices and Skyrmions appear prominently in diverse areas of physics, from cosmology and string theory [1] to QCD, the physics of hadrons, and condensed matter physics [2]. In solid state magnetism alone, topological textures bring together fundamental and applied science, from novel states of matter such as Skyrmion lattice to prototype spintronic devices that employ Skyrmions and domain walls to process information [3]. While early spintronics research largely focussed on ferromagnetic materials [4–6], an ever increasing effort has been turning to antiferromagnets [7, 8] in view of numerous attractive properties arising from shorter characteristic timescales and the absence of net magnetization. Antiferromagnetic Skyrmions have been drawing attention [9, 10] thanks to desirable properties such as lower driving currents and propagation along a straight line.

Here we study a Skyrmion in an antiferromagnetic insulator and show that it creates electron bound states whose energy scale is defined by the gap Δ in the electron spectrum. These bound states turn the Skyrmion into a charged particle, a key result of our work.

We begin with deriving the low-energy electron Hamiltonian for a centrosymmetric Néel antiferromagnet in the presence of a texture. Then we focus on a specific location of the electron band extrema, and a single Skyrmion as texture. We demonstrate the appearance of Skyrmion-electron bound states, and study their evolution as a function of the Skyrmion size. Finally, we discuss the validity range of our results and their implications.

Electron in the presence of a texture — Consider a collinear Néel antiferromagnet on a square-symmetry lattice with period a . Its ordered moment changes sign upon elementary translation, and couples electron states at any two momenta \mathbf{p} and $\mathbf{p} + \mathbf{Q}$, separated by the Néel wave vector $\mathbf{Q} = (\pm\frac{\pi}{a}, \pm\frac{\pi}{a})$. The coupling has the form of exchange $(\Delta \cdot \sigma)$, with Δ proportional to the staggered magnetization, and σ the triad of Pauli matrices, representing electron spin. Since \mathbf{p} and $\mathbf{p} + 2\mathbf{Q}$ are equivalent in the Brillouin zone (BZ), the Hamiltonian \mathcal{H} can be written as acting on a bispinor $\Psi = (\psi_{\mathbf{p}}, \psi_{\mathbf{p}+\mathbf{Q}})$ [11]:

$$\mathcal{H} = \begin{bmatrix} \varepsilon(\mathbf{p}) & (\Delta \cdot \sigma) \\ (\Delta \cdot \sigma) & \varepsilon(\mathbf{p} + \mathbf{Q}) \end{bmatrix}, \quad (1)$$

where $\varepsilon(\mathbf{p})$ is the electron dispersion in the absence

of Néel order. The resulting doubly-degenerate spectrum is $E_{\mathbf{p}} = \varepsilon_+(\mathbf{p}) \pm \sqrt{|\Delta|^2 + \varepsilon_-^2(\mathbf{p})}$, where $\varepsilon_{\pm}(\mathbf{p}) \equiv \frac{1}{2}[\varepsilon(\mathbf{p}) \pm \varepsilon(\mathbf{p} + \mathbf{Q})]$; it has a gap $\Delta = |\Delta|$, which turns a half-filled metal into an insulator.

In the presence of a texture $\Delta_{\mathbf{r}} = \hat{\mathbf{n}}_{\mathbf{r}}\Delta$, with unit vector $\hat{\mathbf{n}}_{\mathbf{r}}$ a smooth function of the coordinate \mathbf{r} , carriers near the extrema of $E_{\mathbf{p}}$ at momenta \mathbf{p}_0 and $\mathbf{p}_0 + \mathbf{Q}$ admit a low-energy effective-mass description [12]. To derive it, in Eq. (1) we replace uniform Δ by $\Delta_{\mathbf{r}}$, and substitute $\hat{\mathbf{p}} \equiv -i\hbar\nabla$ for the momentum dependences $\varepsilon_{\mathbf{p}_0}(\hat{\mathbf{p}})$ and $\varepsilon_{\mathbf{p}_0+\mathbf{Q}}(\hat{\mathbf{p}})$ of $\varepsilon(\mathbf{p})$ near \mathbf{p}_0 and $\mathbf{p}_0 + \mathbf{Q}$.

Now perform a spin rotation $U_{\mathbf{r}}$ that makes $\Delta_{\mathbf{r}}$ uniform: $U_{\mathbf{r}}^\dagger(\hat{\mathbf{n}}_{\mathbf{r}} \cdot \sigma)U_{\mathbf{r}} = \sigma_z$ [13]. This generates a Peierls substitution $\hat{p}_i \rightarrow \hat{p}_i + (\mathbf{A}_i \cdot \sigma)$ in $\varepsilon_{\mathbf{p}_0}(\hat{\mathbf{p}})$ and $\varepsilon_{\mathbf{p}_0+\mathbf{Q}}(\hat{\mathbf{p}})$, with $(\mathbf{A}_i \cdot \sigma) = A_i^\alpha \sigma^\alpha = -i\hbar U_{\mathbf{r}}^\dagger \partial_i U_{\mathbf{r}}$. Vector potential A_i^α carries real-space indices $i = x, y$ and spin indices $\alpha = x, y, z$. While different components of $(\mathbf{A} \cdot \sigma)$ do not commute, $U_{\mathbf{r}}$ is defined only up to a non-uniform spin rotation $V_{\mathbf{r}}^z = e^{i\sigma_z \chi}$ around \hat{z} : $U_{\mathbf{r}} \rightarrow U_{\mathbf{r}} V_{\mathbf{r}}^z$, which is an abelian transformation. This gauge transformation acts on $(\mathbf{A} \cdot \sigma)$ in a peculiar way, elucidated by first-order expansion in infinitesimal χ :

$$\delta(\mathbf{A}_i \cdot \sigma) = \sigma^z \partial_i \chi + \chi [(\mathbf{A}_i \cdot \sigma), \sigma_z]. \quad (2)$$

That is, A_i^z transforms as electromagnetic vector potential ($\delta A_i^z = \partial_i \chi$), while $\mathbf{A}_i^\parallel = (A_i^x, A_i^y)$ rotates around \hat{z} by angle 2χ . This observation will prove useful below.

Next, we split the bispinor Ψ into two spin- $\frac{1}{2}$ components, for energies near $\pm\Delta$, thus taking the 4×4 ('Dirac') Hamiltonian (1) to its 2×2 ('Pauli-Schrödinger') low-energy limit [14, 15]. Here, we focus on the conduction band (energies E near $+\Delta$) and, to first order in $\frac{E-\Delta}{\Delta}$, find the effective low-energy Hamiltonian $\mathcal{H}_{\mathbf{p}_0}$ near \mathbf{p}_0 , with $\bar{\varepsilon}_{\mathbf{p}_0+\mathbf{Q}}(\hat{\mathbf{p}}) \equiv \sigma_z \varepsilon_{\mathbf{p}_0+\mathbf{Q}}(\hat{\mathbf{p}}) \sigma_z$:

$$\mathcal{H}_{\mathbf{p}_0} = \frac{\varepsilon_{\mathbf{p}_0}(\hat{\mathbf{p}}) + \bar{\varepsilon}_{\mathbf{p}_0+\mathbf{Q}}(\hat{\mathbf{p}})}{2} + \frac{[\varepsilon_{\mathbf{p}_0}(\hat{\mathbf{p}}) - \bar{\varepsilon}_{\mathbf{p}_0+\mathbf{Q}}(\hat{\mathbf{p}})]^2}{8\Delta}. \quad (3)$$

The explicit form of Hamiltonian (3) depends on that of $\varepsilon_{\mathbf{p}_0}(\hat{\mathbf{p}})$ and $\varepsilon_{\mathbf{p}_0+\mathbf{Q}}(\hat{\mathbf{p}})$, in its turn defined by the symmetry of momenta \mathbf{p}_0 and $\mathbf{p}_0 + \mathbf{Q}$ in the BZ. Here we focus on the extrema at midpoints Σ of the magnetic Brillouin zone (MBZ) boundary in Fig. 1. The momentum expansion of $\varepsilon_{\mathbf{p}_0}(\hat{\mathbf{p}})$ and $\varepsilon_{\mathbf{p}_0+\mathbf{Q}}(\hat{\mathbf{p}})$ begins with $\pm \mathbf{v} \cdot \hat{\mathbf{p}} + \hat{p}_i^2/2m_i$,

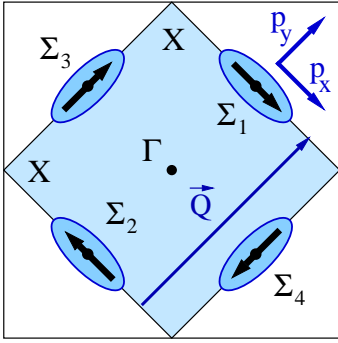


FIG. 1: The Brillouin zone of a square-lattice Néel antiferromagnet with wave vector $\vec{Q} = (\pm\frac{\pi}{a}, \pm\frac{\pi}{a})$. The large square shows the Brillouin zone in the paramagnetic state, the shaded smaller square depicts the Brillouin zone in the Néel state (MBZ). The band extrema are assumed to lie at face centers Σ_1 - Σ_4 of the MBZ. The p_x, p_y are the local momentum axes near Σ_1 , as used in the main text. The ellipses sketch the equal- E_p lines near Σ_1 - Σ_4 . The bold arrows centered at Σ_1 - Σ_4 show the electron spin polarization of the bound state in each valley, for a large BP Skyrmion of Néel type (see main text).

with the paramagnetic-state Fermi velocity \mathbf{v} at Σ pointing along the local p_y in Fig. 1, and $m_i = m_x, m_y$ the paramagnetic-state effective masses along and normal to the MBZ boundary. Truncating the momentum expansion of Eq. (3) at quadratic terms [16], we find

$$\mathcal{H}_\Sigma = \frac{(\hat{p}_i + A_i^z \sigma_z)^2}{2m_i^*} + \frac{(A_i^\parallel)^2}{2m_i} + v(\mathbf{A}_y^\parallel \cdot \boldsymbol{\sigma}). \quad (4)$$

Despite its peculiar appearance, Hamiltonian (4) is gauge-invariant: recall that, by Eq. (2), gauge transformation of \mathbf{A}_i^\parallel amounts to its spin rotation around \hat{z} . Hamiltonian (4) is an extension, to non-planar textures, of the approach used to study planar spiral phases in doped antiferromagnets [17].

Note that m_y^* in Eq. (4) is renormalized relative to m_y in the expansion of $\varepsilon_{\mathbf{p}_0}(\hat{\mathbf{p}})$ and $\varepsilon_{\mathbf{p}_0+\mathbf{Q}}(\hat{\mathbf{p}})$, as per $(m_y^*)^{-1} = (m_y)^{-1} + \frac{v^2}{\Delta}$. Thus, m_y^* is small against m_y : $\frac{m_y^*}{m_y} \sim \frac{\Delta}{\varepsilon_F} \ll 1$, while $m_x^* = m_x$ is of the order of band electron mass m or greater – see Section 1 of Supplemental Material (SM) [18]. Notice that, with only the nearest-neighbor hopping, m_x at Σ is infinite.

A tractable example — Let us turn to Hamiltonian (4) with $(\mathbf{A} \cdot \boldsymbol{\sigma})$ defined by a single Skyrmion. Consider a centrosymmetric isotropic antiferromagnet with stiffness J and continuum-limit energy density $J(\nabla \hat{\mathbf{n}}_r)^2$. In the topological sector with winding number \mathcal{Q} , the lowest-energy solution is the Belavin-Polyakov (BP) Skyrmion [19, 20], defined by its radius R , with R -independent energy $4\pi J\mathcal{Q}$. We are thus lead (see section 2 of [18]) to study Hamiltonian (4) for a $\mathcal{Q} = 1$ BP Skyrmion. We consider a high-symmetry configuration

$\hat{\mathbf{n}}_r = (\sin \theta \cos \phi, \sin \theta \sin \phi, \cos \theta)$ with the polar angle θ of $\hat{\mathbf{n}}_r$ depending only on the distance $r = \sqrt{x^2 + y^2}$ to the Skyrmion center, and $\phi = \arctan \frac{y}{x}$ the azimuthal angle in the (x, y) plane. The energy density above is invariant under shifting ϕ by a constant γ , usually called ‘helicity’ [10]. This allows us to reduce the problem to the $\gamma = 0$ pattern, commonly called the ‘Néel’ Skyrmion.

Note that the latter has its own localized eigenexcitations [21], which, generally, shall be treated on an equal footing with the electron degrees of freedom. However, for a sufficiently small single-ion anisotropy and a not too large BP Skyrmion, the proper Skyrmion frequencies are small against those of electron motion (see section 2 of [18]). We focus on the latter limit and study the electron problem for a static Skyrmion.

We fix the gauge by choosing $U_r = (\mathbf{m}_r \cdot \boldsymbol{\sigma})$, with \mathbf{m}_r along the bisector between \hat{z} and Δ_r . Being a π -rotation around \mathbf{m}_r , such a U_r brings Δ_r to point along \hat{z} [22].

The BP Skyrmion of radius R is defined by $\sin \theta = \frac{2z}{1+z^2}$ with $z = \frac{r}{R}$, so that $\theta[R] = \frac{\pi}{2}$. As a result, the spin- z components A_i^z in the first term of Eq. (4) read

$$A_x^z = \frac{-\hbar y}{R^2 + r^2}, \quad A_y^z = \frac{\hbar x}{R^2 + r^2}. \quad (5)$$

Thus, the Skyrmion produces geometric flux $\pm 2\pi\hbar$ for the spin-up and spin-down components of the wave function: $\oint A_i^z dl_i = 2\pi\hbar$, with the integral taken along a circle, large against R [23]. This flux induces topological spin Hall effect [24–26]. The second term in Eq. (4) creates a repulsive potential

$$\frac{(A_i^\parallel)^2}{2m_i} = \frac{\hbar^2}{2R^2} \left[\frac{1}{m_x} + \frac{1}{m_y} \right] \frac{1}{(1+z^2)^2}, \quad (6)$$

whereas the last term takes the form

$$v(\mathbf{A}_y^\parallel \cdot \boldsymbol{\sigma}) = -\frac{\hbar v}{R} \frac{\sigma^x}{1+z^2}, \quad (7)$$

and thus produces an attractive potential for the spin-up component of the wave function along the \hat{x} axis [27]. Direct inspection shows that, for $R \gg \xi = \frac{\hbar v}{\Delta}$, the r.h.s. of Eq. (7) overwhelms all the other terms with A_i^α in Eq. (4), and creates a Skyrmion-electron bound state, the key result of our work. The bound state is nondegenerate and, at $R \gg \xi$, spin-polarized in each of the four Σ valleys as shown in Fig. 1 [28].

The mass anisotropy $\frac{m_y^*}{m_x^*} \sim \frac{\Delta}{\varepsilon_F} \ll 1$ of Hamiltonian (4) makes the y coordinate ‘fast’ relative to x , and the bound-state energy can be readily evaluated using the Born-Oppenheimer approximation [29]. For $R \gg \xi$, the energy ε_0^e of the lowest bound state, generated by the conduction band, can be evaluated by expanding the r.h.s. of (7) to first order in z^2 and finding the ground state of the ensuing harmonic oscillator with respect to y :

$$\varepsilon_0^e(R) \approx -\Delta \frac{\xi}{R} \left[1 - \frac{1}{\sqrt{2}} \sqrt{\frac{\xi}{R}} \right]. \quad (8)$$

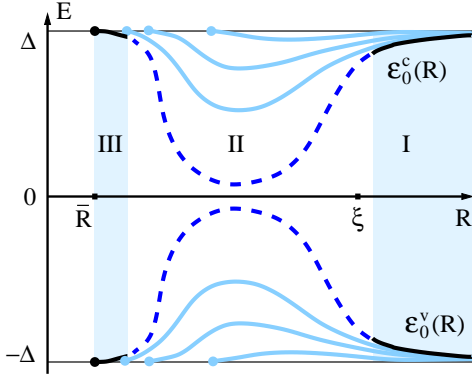


FIG. 2: Energy $\epsilon_0^c(R)$ of BP Skyrmion-electron bound state, generated by the conduction band, and of its valence-band counterpart $\epsilon_0^v(R)$ (the highest filled state), sketched as a function of the BP Skyrmion radius R . **In region I** ($R \gg \xi = \frac{\hbar v}{\Delta}$), the bound state is described by low-energy Hamiltonian (4). The $\epsilon_0^c(R)$ is given by Eq. (8) and shown by solid line. **In region II** ($\bar{R} \ll R \lesssim \xi$), the low-energy approximation breaks down, and the bound state (dashed line) must be found from the full Hamiltonian of a kind (1) in the presence of the Skyrmion, which goes beyond the scope of this work. **In region III** (narrow range $R - \bar{R} \ll \bar{R}$), the bound state, shown by solid line, becomes shallow again. Its disappearance at $R = \bar{R}$ can be described by low-energy Hamiltonian (4) (see main text). Pale lines sketch the higher bound states.

Subsequent account of the ‘slow’ coordinate x introduces only a correction of the order of $\sqrt{\frac{m_y}{m_x}} \sqrt{\frac{a}{\xi}} \ll 1$ to the coefficient $\frac{1}{\sqrt{2}}$ in Eq. (8). For $R \gg \xi$, the bound state (8) is shallow ($|\epsilon_0^c| \ll \Delta$), and the low-energy approximation of Hamiltonians (3) and (4) remains valid. However, with R decreasing, $|\epsilon_0^c|$ grows to attain the order of Δ at $R \sim \xi$, where the low-energy approximation breaks down along with Hamiltonians (3) and (4), as sketched in Fig. 2.

Now we will show that, with R decreasing further below ξ , the bound state becomes shallow again, and vanishes at an $\bar{R} \sim \sqrt{\frac{m_y}{m_x}} \sqrt{\xi a}$. To make this length scale manifest, we eliminate A_y^z from the first term in Eq. (4) by gauge transformation

$$W = e^{i\sigma_z \chi}, \quad \chi(\tilde{x}, \tilde{y}) = \frac{-\tilde{x}}{\sqrt{1+\tilde{x}^2}} \arctan \frac{\tilde{y}}{\sqrt{1+\tilde{x}^2}}, \quad (9)$$

where $\tilde{x} = \frac{x}{R}$ and $\tilde{y} = \frac{y}{R}$. As a result, Hamiltonian (4) takes the form

$$\tilde{\mathcal{H}}_\Sigma = \frac{\hat{p}_y^2}{2m_y^*} + v \left(\tilde{\mathbf{A}}_y^\parallel \cdot \boldsymbol{\sigma} \right) + \frac{\left(A_i^\parallel \right)^2}{2m_i} + \frac{\left(\hat{p}_x + \tilde{A}_x^z \sigma_z \right)^2}{2m_x}, \quad (10)$$

where $\tilde{A}_x^z = A_x^z + \partial_x \chi$, and

$$\left(\tilde{\mathbf{A}}_y^\parallel \cdot \boldsymbol{\sigma} \right) = A_y^\parallel [\sigma^x \cos 2\chi + \sigma^y \sin 2\chi].$$

In terms of the ‘fast’ coordinate y , Hamiltonian (10) describes a particle in a one-dimensional potential $\mathcal{U}_x(y)$,

parametrically dependent on the ‘slow’ variable x , which again invites the Born-Oppenheimer approximation. Comparing the characteristic value $\frac{\hbar v}{R}$ of the second term in Eq. (10) with typical kinetic energy $\frac{\hbar^2}{m_y R^2}$ of the trapped electron, we see that the former is indeed small against the latter for $R \ll \xi$, the range in question. The effective bound-state energy is thus defined by the integrated potential $u(x) = \int \mathcal{U}_x(y) dy$ [30]. Contribution of the second term in Eq. (10) to $u(x)$ is

$$u_1(x) \sigma^x = -v \int dy \left(\tilde{\mathbf{A}}_y^\parallel \cdot \boldsymbol{\sigma} \right) = \hbar v \sigma^x \frac{\sin \left(\frac{\pi \tilde{x}}{\sqrt{1+\tilde{x}^2}} \right)}{\tilde{x}}. \quad (11)$$

The third term in Eq. (10) is an $\frac{a}{R} \ll 1$ fraction of the second, thus its contribution to $u(x)$ can be neglected as long as continuum description of the Skyrmion applies ($R \gg a$). By contrast,

$$u_2(x) = \frac{1}{2m_x} \int dy (\tilde{A}_x^z)^2, \quad (12)$$

arising from the last term, requires care since $(\tilde{A}_x^z)^2$ remains finite as $y \rightarrow \infty$:

$$A^2(x) \equiv \lim_{y \rightarrow \infty} (\tilde{A}_x^z)^2 = \frac{\hbar^2}{R^2} \frac{[\pi/2]^2}{(1+\tilde{x}^2)^3},$$

which makes $u_2(x)$ diverge. We remedy this by writing $(\tilde{A}_x^z)^2 = [(\tilde{A}_x^z)^2 - A^2(x)] + A^2(x)$. The term in the square brackets then gives a finite contribution to $u(x)$, which is suppressed relative to $u_1(x)$ by a factor $\frac{m_y a}{m_x R}$, and hence negligible within continuum description ($R \gg a$). The resulting bound-state energy $w_-(x)$ at a given x is thus defined [30] by $u_1(x)$ alone:

$$w_-(x) = -\frac{m_y^*}{2\hbar^2} [u_1(x)]^2 = -\frac{\Delta}{2} \frac{\sin^2 \left(\frac{\pi \tilde{x}}{\sqrt{1+\tilde{x}^2}} \right)}{\tilde{x}^2}. \quad (13)$$

It competes with the repulsive contribution of $A^2(x)$:

$$w_+(x) = \frac{A^2(x)}{2m_x} = \frac{\hbar^2}{2m_x R^2} \frac{[\pi/2]^2}{(1+\tilde{x}^2)^3}. \quad (14)$$

As per Eqs. (5) and (9), \tilde{A}_x^z is odd with respect to y , thus the cross-term $\left\{ \hat{p}_x, \tilde{A}_x^z \sigma_z \right\} / 2m_x$ averages out upon integration over y . Upon switching to the dimensionless coordinate $\tilde{x} = \frac{x}{R}$, the resulting Hamiltonian $\tilde{\mathcal{H}}_x$ reads

$$\tilde{\mathcal{H}}_x = \frac{\hbar^2}{2m_x R^2} \left[-\frac{d^2}{d\tilde{x}^2} + \frac{[\pi/2]^2}{(1+\tilde{x}^2)^3} \right] - \frac{\Delta}{2} \frac{\sin^2 \left[\frac{\pi \tilde{x}}{\sqrt{1+\tilde{x}^2}} \right]}{\tilde{x}^2}. \quad (15)$$

Taken alone, the last term above is obviously beyond the low-energy approximation. However, with decreasing R , the repulsion grows relative to attraction, and overcomes it at an $\bar{R} \sim \sqrt{\frac{m_y}{m_x}} \sqrt{\xi a} \ll \xi$. Thus, Hamiltonian (15)

is valid only in a narrow range $R - \bar{R} \ll \bar{R}$, where the bound state becomes shallow to disappear at $R = \bar{R}$. Notice that $\bar{R} \gg a$ as long as the ratio $\frac{m_y}{m_x}$ is not too small ($\frac{m_y}{m_x} \gg \frac{\Delta}{\epsilon_F}$).

Note that neither the bound state becoming shallow in a narrow range near \bar{R} nor its disappearance at \bar{R} rely on the mass anisotropy: the same behavior obtains for a perfectly isotropic mass, where the Hamiltonian can be diagonalized by solving a single equation for the radial wave function.

Together with Eq. (8), this behavior has several implications, that we illustrate at half-filling. The total number of states (itinerant plus bound) generated by the valence band in the presence of the Skyrmion equals the number of electrons – that is, the number of unit cells in the sample. At the same time, by particle-hole symmetry, every bound state $\epsilon_\alpha^c(R)$, split from the conduction band, has a valence-band counterpart $\epsilon_\alpha^v(R) = -\epsilon_\alpha^c(R)$, as shown in Fig. 2. Therefore, at $T = 0$, all the negative-energy states are filled, while all the positive-energy states are empty. Qualitatively, the energy $\epsilon_0^v(R)$ of the highest filled state behaves as sketched in Fig. 2.

Discussion and conclusions — We have shown that, in a Néel antiferromagnet with a specific location of the electron band extrema, a Skyrmion produces electron bound states and becomes charged. The effect does not rely on the BP profile we used as an illustration, and appears for *any* credible shape such as that of a domain-wall Skyrmion.

The Skyrmion-electron bound states owe their existence to the texture-induced spin-orbit coupling, the last term in Eq. (4). The latter arises from Néel order, and has no equivalent in a ferromagnet. At the same time, the said term hinges on the lower symmetry of Σ points in the Brillouin zone: at the corner points X or at the center point Γ in Fig. 1, such a term is not allowed. Note that, unlike the textbook spin-orbit coupling arising from the Pauli term in the Schrödinger Hamiltonian, the texture-induced spin-orbit term in Eq. (4) does not involve the fine structure constant $\alpha = \frac{e^2}{\hbar c}$ at all, and is small (relative to Δ) only in the measure of the texture being large against the Néel coherence length $\xi = \frac{\hbar v}{\Delta}$.

As we have shown, the Skyrmion-electron bound state is nondegenerate, with the energy scale defined by the gap Δ in the electron spectrum in the Néel state. In this regard, the texture-induced spin-orbit coupling in Eq. (4) is similar to band splitting effects of the same scale, found in certain types of antiferromagnets [31–34].

The Skyrmion-electron bound state is a new arrival in the family of electron states, localized on topological defects such as dislocations [35], vortices in superconductors [36] or solitons in organic materials [37, 38]. In addition to its fundamental interest, charged Skyrmion can be manipulated by electric field, which may open new possibilities for its use in devices. We hope that our

results stimulate further work both on fundamental and applied aspects of this phenomenon.

We thank P. Pujol for the many discussions, helpful suggestions and enlightening remarks. We are grateful to Ya. Bazaliy and to M. Kartsovnik for illuminating comments. Finally, we thank G. Baskaran for pointing us, after this work appeared on the arXiv, to early work [39, 40] that studied Skyrmion-electron bound states in an exotic spin liquid state of the Hubbard model (see section 3 of [18]).

* davier@irsamc.ups-tlse.fr

† revaz@irsamc.ups-tlse.fr

- [1] K. Becker, M. Becker, and J. H. Schwarz, *String Theory and M-Theory* (Cambridge University Press, Cambridge, 2007).
- [2] M. Rho and I. Zahed (Eds.), *The Multifaceted Skyrmion* (World Scientific, 2016)
- [3] C. Back *et al.*, J. Phys. D: Appl. Phys. **53**, 363001 (2020).
- [4] A. Fert, Rev. Mod. Phys. **80**, 1517 (2008).
- [5] P. A. Grünberg, Rev. Mod. Phys. **80**, 1531 (2008).
- [6] A. Fert, F. N. V. Dau, C. R. Physique **20**, 817 (2019).
- [7] O. Gomonay, T. Jungwirth, and J. Sinova, Phys. Status Solidi RRL, **11**: 1700022 (2017).
- [8] V. Baltz, A. Manchon, M. Tsoi, T. Moriyama, T. Ono, Y. Tserkovnyak Rev. Mod. Phys. **90**, 015005 (2018).
- [9] L. Šmejkal, Yu. Mokrousov, B. Yan, and A. H. MacDonald, Nature Phys. **14**, 242 (2018).
- [10] B. Göbel, I. Mertig, O. A. Tretiakov, Phys. Rep. **895**, 1 (2021).
- [11] N. I. Kulikov and V. V. Tugushev, Usp. Fiz. Nauk **144**, 643 (1984) [Sov. Phys. Usp. **27**, 954 (1984)].
- [12] C. Kittel, *Quantum Theory of Solids* (John Wiley & Sons, Inc., New York – London, 1963).
- [13] G. E. Volovik, J. Phys. C: Solid State Phys. **20**, L83 (1987).
- [14] V. B. Berestetskii, E. M. Lifshitz and L. P. Pitaevskii, “Course of Theoretical Physics”, Vol. 4, *Quantum Electrodynamics* (Pergamon Press, Oxford, 1982).
- [15] L. H. Ryder, *Quantum Field Theory* (Cambridge University Press, Cambridge, 1996).
- [16] The terms omitted when passing from Eq. (3) to (4) are higher order in momentum. They are negligible as long as the low-energy approximation of Eqs. (3-4) is valid.
- [17] B. I. Shraiman, E. D. Siggia, Phys. Rev. Lett. **62**, 1564 (1989).
- [18] See Supplemental Material at [URL to be provided by the publisher] for a discussion (i) of mass anisotropy at point Σ in topical materials, and (ii) of the parameter range, where the BP Skyrmion illustration is relevant, and (iii) for a brief comparison of our results with those of Refs. [39, 40]. The Supplemental Material also includes Refs. [41–59].
- [19] A. A. Belavin and A. M. Polyakov, Pis'ma Zh. Eksp. Teor. Fiz. **22**, 503 (1975) [JETP Lett. **22**, 245 (1975)].
- [20] R. Rajaraman, *Solitons and Instantons* (North-Holland, Amsterdam, 1989).
- [21] V. P. Kravchuk, O. Gomonay, D. D. Sheka, D. R. Rodrigues, K. Everschor-Sitte, J. Sinova, J. van den Brink,

- and Yu. Gaididei, Phys. Rev. B **99**, 184429 (2019).
- [22] G. Tatara, H. Kohno, and J. Shibata, Phys. Rep. **468**, 213 (2008).
- [23] This is true for *any* $Q = 1$ Skyrmion profile. For an arbitrary Q , the corresponding flux is $\pm 2\pi Q$.
- [24] G. Yin, Y. Liu, Y. Barlas, J. Zang, and R. K. Lake, Phys. Rev. B **92**, 024411 (2015).
- [25] P. M. Buhl, F. Freimuth, S. Blügel, and Yu. Mokrousov, Phys. Status Solidi RRL, **11**: 1700007 (2017).
- [26] C. A. Akosa, O. A. Tretiakov, G. Tatara, and A. Manchon, Phys. Rev. Lett. **121**, 097204 (2018).
- [27] The strikingly simple r.h.s. of Eq. (7) is a remarkable property of the BP Skyrmion.
- [28] For chirality $\gamma \neq 0$, spin polarization of the bound state is tilted by γ relative to the local \hat{x} axis in Fig. 1.
- [29] J. C. Tully, Perspective on “Zur Quantentheorie der Molekeln”. In: Cramer C.J., Truhlar D.G. (eds) *Theoretical Chemistry Accounts* (Springer, Berlin, Heidelberg, 2000).
- [30] L. D. Landau and E. M. Lifshitz, “Course of Theoretical Physics”, Vol. 3, *Quantum Mechanics, Non-relativistic Theory* (Pergamon Press, Oxford, 1991).
- [31] S. I. Pekar and E. I. Rashba, Zh. Eksp. Teor. Fiz. **47**, 1927 (1964) [Sov. Phys. JETP **20**, 1295 (1965)].
- [32] S. Hayami, Y. Yanagi, and H. Kusunose, J. Phys. Soc. Jpn. **88**, 123702 (2019).
- [33] L-D. Yuan, Z. Wang, J-W. Luo, E. I. Rashba, and A. Zunger, Phys. Rev. B **102**, 014422 (2020).
- [34] H. Reichlová, R. L. Seeger, R. González-Hernández, I. Kounta, R. Schlitz, D. Krieger, P. Ritzinger, M. Lamme, M. Leiviskä, V. Petříček, P. Doleál, E. Schmoranzarová, A. Bad’ura, A. Thomas, V. Baltz, L. Michez, J. Sinova, S. T. B. Goennenwein, T. Jungwirth, L. Šmejkal, arXiv:2012.15651.
- [35] R. Landauer, Phys. Rev. **94**, 1386 (1954).
- [36] C. Caroli, P. G. De Gennes, J. Matricon, Phys. Lett. **9**, 307 (1964).
- [37] S. A. Brazovskii and N. N. Kirova, Sov. Sci. Rev. A **5**, 99 (1984).
- [38] A. J. Heeger, S. Kivelson, J. R. Schrieffer, and W. -P. Su, Rev. Mod. Phys. **60**, 781 (1988).
- [39] S. John, A Golubentsev, Phys. Rev. Lett. **71**, 3343 (1993).
- [40] S. John, A Golubentsev, Phys. Rev. B **51**, 381 (1995).
- [41] N. P. Armitage, F. Ronning, D. H. Lu, C. Kim, A. Damascelli, K. M. Shen, D. L. Feng, H. Eisaki, Z.-X. Shen, P. K. Mang, N. Kaneko, M. Greven, Y. Onose, Y. Taguchi, and Y. Tokura, Phys. Rev. Lett. **88**, 257001 (2002).
- [42] H. Matsui, T. Takahashi, T. Sato, K. Terashima, H. Ding, T. Uefuji, and K. Yamada, Phys. Rev. B **75**, 224514 (2007).
- [43] D. Song, G. Han, W. Kyung, J. Seo, S. Cho, B. S. Kim, M. Arita, K. Shimada, H. Namatame, M. Taniguchi, Y. Yoshida, H. Eisaki, S. R. Park, and C. Kim, Phys. Rev. Lett. **118**, 137001 (2017).
- [44] G. M. Luke, L. P. Le, B. J. Sternlieb, Y. J. Uemura, J. H. Brewer, R. Kadono, R. F. Kiefl, S. R. Kreitzman, T. M. Riseman, C. E. Stronach, M. R. Davis, S. Uchida, H. Takagi, Y. Tokura, Y. Hidaka, T. Murakami, J. Gopalakrishnan, A. W. Sleight, M. A. Subramanian, E. A. Early, J. T. Markert, M. B. Maple, and C. L. Seaman, Phys. Rev. B **42**, 7981 (1990).
- [45] E. M. Motoyama, G. Yu, I. M. Vishik, O. P. Vajk, P. K. Mang, and M. Greven, Nature **445**, 186 (2007).
- [46] P. K. Mang, S. Larochelle, A. Mehta, O. P. Vajk, A. S. Erickson, L. Lu, W. J. L. Buyers, A. F. Marshall, K. Prokes, and M. Greven, Phys. Rev. B **70**, 094507 (2004).
- [47] H. Saadaoui, Z. Salman, H. Luetkens, T. Prokscha, A. Suter, W. A. MacFarlane, Y. Jiang, K. Jin, R. L. Greene, E. Morenzoni, and R. F. Kiefl, Nat. Commun. **6**, 6041 (2015).
- [48] K. Yamada, K. Kurahashi, T. Uefuji, M. Fujita, S. Park, S.-H. Lee, and Y. Endoh, Phys. Rev. Lett. **90**, 137004 (2003).
- [49] H. J. Kang, P. Dai, H. A. Mook, D. N. Argyriou, V. Sikolenko, J. W. Lynn, Y. Kurita, S. Komiya, and Y. Ando, Phys. Rev. B **71**, 214512 (2005).
- [50] Y. Dagan, M. C. Barr, W. M. Fisher, R. Beck, T. Dhakal, A. Biswas, and R. L. Greene, Phys. Rev. Lett. **94**, 057005 (2005).
- [51] W. Yu, J. S. Higgins, P. Bach, and R. L. Greene, Phys. Rev. B **76**, 020503(R) (2007).
- [52] A. Dorantes, A. Alshemi, Z. Huang, A. Erb, T. Helm, and M. V. Kartsovnik, Phys. Rev. B **97**, 054430 (2018).
- [53] R. Ramazashvili, P. D. Grigoriev, T. Helm, F. Kollmannsberger, M. Kunz, W. Biberacher, E. Kampert, H. Fujiwara, A. Erb, J. Wosnitza, R. Gross, and M. V. Kartsovnik npj Quantum Mater. **6**, 11 (2021).
- [54] C. Kittel, Phys. Rev. **82**, 565 (1951).
- [55] S. M. Rezende, A. Azevedo, and R. L. Rodríguez-Suárez, J. Appl. Phys. **126**, 151101 (2019).
- [56] T. Mori and M. Katsuhara, Journ. Phys. Soc. Japan, **71**, 826 (2002).
- [57] V. P. Voronov, B. A. Ivanov, and A. M. Kosevich, Zh. Eksp. Teor. Fiz. **84**, 2235 (1983) [Sov. Phys. JETP **57**, 1303 (1983)].
- [58] A. Bogdanov, A. Hubert, J. Magn. Magn. Mater. **138**, 255 (1994).
- [59] A. N. Bogdanov, U. K. Röbber, M. Wolf, and K.-H. Müller, Phys. Rev. B **66**, 214410 (2002).

Supplemental Material to “Skyrmion-electron bound states in a Néel antiferromagnet”

N. Davier^{1,*} and R. Ramazashvili^{1,†}

¹*Laboratoire de Physique Théorique,
Université de Toulouse, CNRS, UPS, France*

(Dated: today)

* davier@irsamc.ups-tlse.fr

† revaz@irsamc.ups-tlse.fr

1. *Mass anisotropy:*

Such a mass anisotropy arises for *any* (not only Néel) $(\frac{\pi}{a}, \frac{\pi}{a})$ order with a gap $\Delta \ll \epsilon_F \equiv mv^2$. Electron-doped cuprates at low-to-optimal doping provide a prominent example [S1–S3], even if the nature of their ordering remains controversial, with experimental evidence presented both against [S4–S7] and for [S8–S13] the presence of (quasi)static Néel order.

2. *The validity range of the BP Skyrmion illustration:*

2.a *When can one treat the BP Skyrmion as static?*

For $R \gtrsim \xi$, treating the BP Skyrmion profile as static input to the electron problem requires the bound-state level spacing $\hbar\omega_e \sim \Delta \left(\frac{\xi}{R}\right)^{\frac{3}{2}}$ in Eq. (8) being large against the energies of high-frequency localized eigenmodes of the Skyrmion. These have no marked dependence on R , and are bound from above by the spin wave gap $\hbar\Omega_0$ of the bulk magnon spectrum [S14]. In the relevant limit $K \ll J$, the behavior $\hbar\Omega_0 \sim \sqrt{KJ}$ [S15, S16] translates the condition $\omega_e \gg \Omega_0$ into $\Delta \left(\frac{\xi}{R}\right)^{3/2} \gg \sqrt{KJ}$. Which means that, at a sufficiently large R , the BP Skyrmion can no longer be treated as static. For a weak enough anisotropy, this limits our treatment to radia

$$R \ll \xi \left(\frac{\Delta}{J}\right)^{2/3} \left(\frac{J}{K}\right)^{1/3}. \quad (\text{S1})$$

Inequality (S1) is meaningful only if its r.h.s. is large compared with ξ , that is if

$$\frac{K}{J} \ll \left(\frac{\Delta}{J}\right)^2. \quad (\text{S2})$$

Now, the conditions (S1,S2) define the possibility of treating the Skyrmion as static when working with y , the ‘fast’ degree of freedom of the electron. For the ‘slow’ coordinate, x , the relevant frequency is $\hbar\omega_e^y \sim \Delta \sqrt{\frac{m_y}{m_x}} \sqrt{\frac{a}{\xi}} \left(\frac{\xi}{R}\right)^{\frac{3}{2}} \ll \hbar\omega_e$, and the conditions for treating the Skyrmion as static when working with the ‘slow’ electron coordinate x are more stringent than (S1):

$$R \ll \xi \left(\frac{\Delta}{\epsilon_F}\right)^{1/3} \left(\frac{m_y}{m_x}\right)^{1/3} \left(\frac{\Delta}{J}\right)^{2/3} \left(\frac{J}{K}\right)^{1/3}. \quad (\text{S3})$$

Inequality (S3) makes sense only if its r.h.s. is large compared with ξ , that is if

$$\frac{K}{J} \ll \left(\frac{\Delta}{J}\right)^2 \frac{m_y}{m_x} \frac{\Delta}{\epsilon_F}. \quad (\text{S4})$$

2.b When is the BP Skyrmion profile relevant in terms of K and D ?

We studied the Skyrmion-electron bound states in a perfectly isotropic and centrosymmetric Néel antiferromagnet, whereas in a realistic solid-state device, the presence of a substrate would give rise to single-ion anisotropy K and Dzyaloshinskii-Moriya coupling D . Here, we inquire about the range of K and D , for which the Belavin-Polyakov Skyrmion picture remains relevant.

Firstly, the bound-state energy scale $|\epsilon_0^c(R)| \sim \Delta \frac{\xi}{R}$ of a medium-to-large ($R \gtrsim \xi$) Belavin-Polyakov (BP) Skyrmion in Eq. (8) must be small against the BP Skyrmion energy $4\pi J$: otherwise, the bound state may favor a different profile. At $R \sim \xi$, this implies

$$\Delta \ll 4\pi J. \quad (\text{S5})$$

Inequality (S5) is favored by the factor 4π in front of J , and by $J \propto S^2$ versus $\Delta \propto S$ scaling with the ordered moment S ; it appears to hold in materials, where estimates have been made [S17].

At the same time, it is necessary that the single-ion anisotropy contribution E_a to the Skyrmion energy \mathcal{W} be small against both the bound-state energy $|\epsilon_0^c(R)| \sim \Delta \frac{\xi}{R}$ and $4\pi J$. The E_a reads

$$E_a = K \int \frac{d^2\mathbf{r}}{a^2} [1 - n_z^2],$$

and thus $E_a \propto K \left(\frac{R}{a}\right)^2$ [S18, S19]. Which, in turn, implies

$$R \ll \xi \left(\frac{\Delta}{\epsilon_F}\right)^{2/3} \left(\frac{\Delta}{K}\right)^{1/3}. \quad (\text{S6})$$

Similarly to inequality (S1), the bound (S6) is meaningful only if its r.h.s. is large compared with ξ , that is if

$$\frac{K}{J} \ll \frac{\Delta}{J} \left(\frac{\Delta}{\epsilon_F}\right)^2. \quad (\text{S7})$$

Comparison of (S2), (S4) and (S7) shows that the latter tends to be more stringent, and thus it is the inequalities (S6) and (S7) that tend to define the BP Skyrmion radii R and the single-ion anisotropy K for which (i) the BP Skyrmion profile can be treated as static input to the electron problem, and (ii) the single-ion anisotropy can be neglected.

Now, the Dzyaloshinskii-Moriya (DM) contribution

$$E_{DM} = D \int \frac{d^2\mathbf{r}}{a} (\hat{\mathbf{n}} \cdot \nabla \times \hat{\mathbf{n}}) \quad (\text{S8})$$

to \mathcal{W} must also be small against both the bound-state energy $|\epsilon_0^c(R)| \sim \Delta \frac{\xi}{R}$ and $4\pi J$. Eq. (S8) shows that $E_{DM} \propto D \frac{R}{a}$. Thus, for sufficiently large R , the DM contribution cannot be neglected. The condition $E_{DM} \ll |\epsilon_0^c(R)|$ thus yields an upper bound for the Skyrmion radii

$$R \ll \xi \frac{\Delta}{\sqrt{\epsilon_F D}}. \quad (\text{S9})$$

Just as the bound (S1), inequality (S9) makes sense only if its r.h.s. is large compared with ξ , that is if

$$\frac{D}{J} \ll \frac{\Delta}{J} \frac{\Delta}{\epsilon_F}. \quad (\text{S10})$$

Finally, K and D must be far from the transition line $D = D_c(K, J)$ between the uniform and the modulated state [S20, S21]:

$$\frac{D}{J} \ll \frac{4}{\pi} \sqrt{\frac{K}{J}}. \quad (\text{S11})$$

Combining the constraints above, we conclude that our treatment of the BP Skyrmion profile is relevant for Skyrmion radii below the smaller of the two bounds (S6) and (S9), while K and D must satisfy the bounds (S7), (S10), and (S11). In other words, these conditions allow one to treat the BP Skyrmion profile as static input to the electron problem, while neglecting the single-ion anisotropy and the DM coupling.

3. Comparison with the early work [S22, S23] by S. John and A. Golubentsev:

It is instructive to compare our results with those of the early work [S22, S23] by S. John and A. Golubentsev, who studied the two-dimensional Hubbard model in a topological spin liquid state, defined by two key properties: (i) checkerboard Néel order, and (ii) anti-periodicity of the electron wave function along closed path around any elementary plaquette of the square lattice. As a consequence, the unit cell in such a state quadruples relative to the underlying square lattice, and the electron wave function is thus a 4-spinor. The model band extrema fall at the very same points $\Sigma = (\pm \frac{\pi}{a}, \pm \frac{\pi}{a})$ that we focussed on, and all the four points Σ are equivalent in the ‘ordered’ Brillouin zone. The resulting ‘Dirac’ electron spectrum near Σ is thus isotropic by symmetry.

As opposed to the above, in the Néel state of our interest the unit cell doubles rather than quadruples, and the electron wave function is thus a bispinor. Contrary to being

all equivalent in the spin liquid state, in the Néel state the four points Σ split into two inequivalent pairs $\Sigma_{1,2}$ and $\Sigma_{3,4}$, shown in Fig. 1. In contrast to the spin-liquid state, the symmetry of the Néel state does not require the electron spectrum near the Σ points to be isotropic, consistently with experimental findings [S1–S3] in a number of cuprates.

Last but not the least, the Skyrmion-electron bound states we found are non-degenerate and spin-polarized in each of the four Σ -valleys as shown in Fig. 1, whereas the bound states found by John and Golubentsev are doubly degenerate as a consequence of the elevated symmetry of the said spin-liquid state [S22, S23].

To summarize, the similarities between the Skyrmion-electron bound states that we studied and those found by John and Golubentsev arise from Néel order being an ingredient of the spin liquid [S22, S23]. The differences stem from the features that are not inherent to a generic Néel state of our interest, such as (i) an elevated symmetry of the spin liquid, and (ii) the wave function antiperiodicity under translation around any elementary plaquette of the square lattice. We hope that our results prove relevant to some of the quasi-two-dimensional antiferromagnets with band electrons.

-
- [S1] N. P. Armitage, F. Ronning, D. H. Lu, C. Kim, A. Damascelli, K. M. Shen, D. L. Feng, H. Eisaki, Z.-X. Shen, P. K. Mang, N. Kaneko, M. Greven, Y. Onose, Y. Taguchi, and Y. Tokura,
- [S2] H. Matsui, T. Takahashi, T. Sato, K. Terashima, H. Ding, T. Uefuji, and K. Yamada, *Phys. Rev. B* **75**, 224514 (2007).
- [S3] D. Song, G. Han, W. Kyung, J. Seo, S. Cho, B. S. Kim, M. Arita, K. Shimada, H. Namatame, M. Taniguchi, Y. Yoshida, H. Eisaki, S. R. Park, and C. Kim, *Phys. Rev. Lett.* **118**, 137001 (2017).
- [S4] G. M. Luke, L. P. Le, B. J. Sternlieb, Y. J. Uemura, J. H. Brewer, R. Kadono, R. F. Kiefl, S. R. Kreitzman, T. M. Riseman, C. E. Stronach, M. R. Davis, S. Uchida, H. Takagi, Y. Tokura, Y. Hidaka, T. Murakami, J. Gopalakrishnan, A. W. Sleight, M. A. Subramanian, E. A. Early, J. T. Markert, M. B. Maple, and C. L. Seaman, *Phys. Rev. B* **42**, 7981 (1990).
- [S5] E. M. Motoyama, G. Yu, I. M. Vishik, O. P. Vajk, P. K. Mang, and M. Greven, *Nature* **445**, 186 (2007).

- [S6] P. K. Mang, S. Larochelle, A. Mehta, O. P. Vajk, A. S. Erickson, L. Lu, W. J. L. Buyers, A. F. Marshall, K. Prokes, and M. Greven, *Phys. Rev. B* **70**, 094507 (2004).
- [S7] H. Saadaoui, Z. Salman, H. Luetkens, T. Prokscha, A. Suter, W. A. MacFarlane, Y. Jiang, K. Jin, R. L. Greene, E. Morenzoni, and R. F. Kiefl, *Nat. Commun.* **6**, 6041 (2015).
- [S8] K. Yamada, K. Kurahashi, T. Uefuji, M. Fujita, S. Park, S.-H. Lee, and Y. Endoh, *Phys. Rev. Lett.* **90**, 137004 (2003).
- [S9] H. J. Kang, P. Dai, H. A. Mook, D. N. Argyriou, V. Sikolenko, J. W. Lynn, Y. Kurita, S. Komiya, and Y. Ando, *Phys. Rev. B* **71**, 214512 (2005).
- [S10] Y. Dagan, M. C. Barr, W. M. Fisher, R. Beck, T. Dhakal, A. Biswas, and R. L. Greene, *Phys. Rev. Lett.* **94**, 057005 (2005).
- [S11] W. Yu, J. S. Higgins, P. Bach, and R. L. Greene, *Phys. Rev. B* **76**, 020503(R) (2007).
- [S12] A. Dorantes, A. Alshemi, Z. Huang, A. Erb, T. Helm, and M. V. Kartsovnik, *Phys. Rev. B* **97**, 054430 (2018).
- [S13] R. Ramazashvili, P. D. Grigoriev, T. Helm, F. Kollmannsberger, M. Kunz, W. Biberacher, E. Kampert, H. Fujiwara, A. Erb, J. Wosnitza, R. Gross, and M. V. Kartsovnik *npj Quantum Mater.* **6**, 11 (2021).
- [S14] V. P. Kravchuk, O. Gomonay, D. D. Sheka, D. R. Rodrigues, K. Everschor-Sitte, J. Sinova, J. van den Brink, and Yu. Gaididei, *Phys. Rev. B* **99**, 184429 (2019).
- [S15] C. Kittel, *Phys. Rev.* **82**, 565 (1951).
- [S16] S. M. Rezende, A. Azevedo, and R. L. Rodríguez-Suárez, *J. Appl. Phys.* **126**, 151101 (2019).
- [S17] T. Mori and M. Katsuhara, *Journ. Phys. Soc. Japan*, **71**, 826 (2002).
- [S18] In this crude estimate, we omit subleading logarithmic enhancement factors [S19].
- [S19] V. P. Voronov, B. A. Ivanov, and A. M. Kosevich, *Zh. Eksp. Teor. Fiz.* **84**, 2235 (1983) [*Sov. Phys. JETP* **57**, 1303 (1983)].
- [S20] A. Bogdanov, A. Hubert, *J. Magn. Magn. Mater.* **138**, 255 (1994).
- [S21] A. N. Bogdanov, U. K. Rößler, M. Wolf, and K.-H. Müller, *Phys. Rev. B* **66**, 214410 (2002).
- [S22] S. John, A Golubentsev, *Phys. Rev. Lett.* **71**, 3343 (1993).
- [S23] S. John, A Golubentsev, *Phys. Rev. B* **51**, 381 (1995).